Journal of Energy and Power Engineering 8 (2014) 785-793

Development of an Evaluation Methodology for Fuel Discharge in Core Disruptive Accidents of Sodium-Cooled Fast Reactors

Kenji Kamiyama, Yoshiharu Tobita, Tohru Suzuki and Ken-ichi Matsuba

Japan Atomic Energy Agency, Ibaraki 311-1393, Japan

Received: December 25, 2013 / Accepted: January 13, 2014 / Published: May 31, 2014.

Abstract: The purpose of the present study is to develop a methodology to evaluate fuel discharge through the CRGT (control-rod guide tube) during CDAs (core-disruptive accidents) of SFRs (sodium-cooled fast reactors), since fuel discharge will decrease the core reactivity and CRGTs have a potential to provide an effective discharge path. Fuel discharge contains multi-component fluid dynamics with phase changes, and, in the present study, the SFR safety analysis code SIMMER (Sn, implicit, multifield, multicomponent, Eulerian recriticality) was utilized as a technical basis. First, dominant phenomena affecting fuel discharge through the CRGT are identified based on parametric calculations by the SIMMER code. Next, validations on the code models closely relating to these phenomena were carried out based on experimental data. It was shown that the SIMMER code with some model modifications could reproduce the experimental results appropriately. Through the present study, the evaluation methodology for the molten-fuel discharge through the CRGT was successfully developed.

Key words: Sodium-cooled fast reactor, core disruptive accident; molten-fuel discharge, FBR (fast breeder reactor) safety analysis code SIMMER.

1. Introduction

One of major concerns in the safety of SFRs (sodium-cooled fast reactors) have been the possibility of recriticality and the resultant energetics potential in the case of postulated CDAs (core disruptive accidents) since an SFR cores are not characteristically arranged in their most reactive configuration and it might exceed prompt criticality under hypothetical degraded-core conditions [1]. Based on this background, although the frequency of CDAs occurrence in SFR is regarded as negligible in an engineering stand point by understandings of initiating events leading to the CDA and developmental efforts for systems to prevent such initiating events, consequences of CDA have been evaluated since energetic events during CDA might affect integrity of the reactor vessel.

The typical initiator leading to the CDA in SFRs is ULOF (unprotected loss-of-flow) in which failure of the reactor scram is assumed in case of trips of all the primary-coolant pumps [2]. ULOF brings sodium boiling in the core region and this boiling inserts the positive reactivity. If the core reactivity does not exceed the prompt criticality by insertion of sodium void reactivity, the core will melt gradually. However, as illustrated in Fig. 1, the progression of core melting and the formation of the large-scale molten-fuel pool in the core region is one of factors leading to energetics, and therefore, discharge of molten-fuel from the core region in the early phase of CDA is effective to eliminate potential of such energetics. Therefore, a methodology for evaluating molten-fuel discharge behavior is required to realistically evaluate sequences

Corresponding author: Kenji Kamiyama, Ph.D., research fields: nuclear safety engineering and thermal-hydraulics in core-disruptive accidents of sodium-cooled fast reactors. E-mail: kamiyama.kenji@jaea.go.jp.

and consequences of CDAs.

Under the ULOF condition, there are three potential fuel-discharge paths in a SFR core design: the first is the intra-subassembly pin-bundle in the axial blanket regions; the second is the inter-subassembly gap channel in the axial and radial blanket regions; and the third is the CRGT (control-rod guide tube). Of these, the CRGT is considered as the most effective discharge path to reduce the core reactivity since its hydraulic diameter is the largest among the three paths.

The purpose of the present study is to develop a methodology to evaluate sequence of molten-fuel discharge through the CRGT. A supposed sequence of molten-fuel discharge through the CRGT is illustrated in Fig. 2, which will be multi-phase, multi-component fluid dynamics with phase changes such as vaporization of coolant, solidification of fuel. In the present study, the SIMMER-III code [3-5], which has been developed to evaluate sequence and consequence of CDA, was utilized as a technical basis since this code is designed to simulate the multi-phase, multi-component fluid dynamics with phase changes which are supposed to take place around the CRGT. First, dominant phenomena which affect fuel discharge through the CRGT are identified based on parametric calculations by the SIMMER-III code. Next, validations on the code models closely relating to identified phenomena were performed based on experimental data.

2. SIMMER-III Application to Fuel-Discharge through the Control Rod Guide Tube

2.1 Procedure of Calculations

The supposed phenomena during molten-fuel discharge as shown in Fig. 2 are transient behavior and require great computational loads for calculations in general. In order to perform calculations efficiently for identifying dominant phenomena to fuel discharge, 2D configuration was applied to the present calculation, as shown in Fig. 3, where the calculation geometry

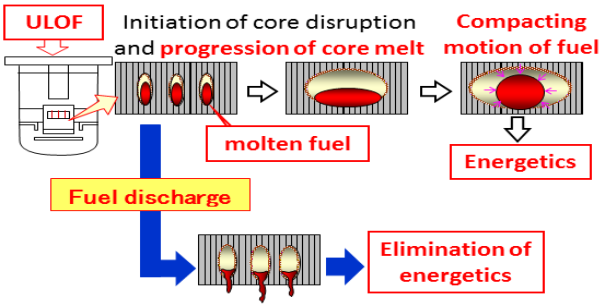

Fig. 1 Schematics of an event sequence for CDA.

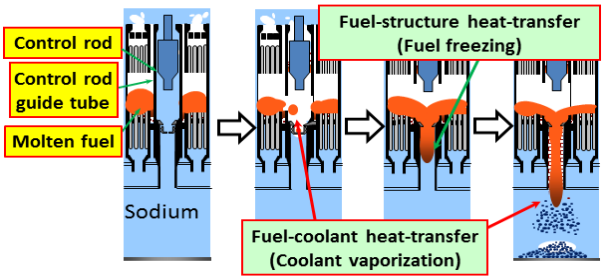

Fig. 2 Supposed sequence of molten-fuel discharge through the CRGT.

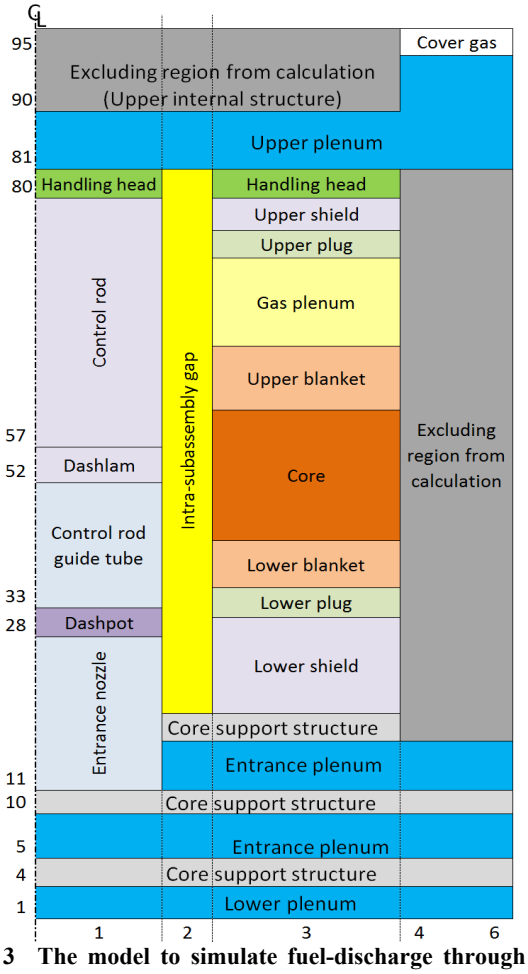

Fig. 3 The model to simulate fuel-discharge through the CRGT.

consists of the CRGT at the center and six fuel subassemblies surrounding the CRGT. Pressure conditions for inlet coolant plenums were set so as to simulate rated coolant-flows for the fuel subassemblies and the CRGT. ULOF was simulated by reducing the pressure conditions for the inlet coolant plenums. At the onset of coolant boiling, the reactor power was set to increase rapidly at sixty-fold of the rated power in order to simulate fuel melting by insertion of the positive reactivity.

2.2 Results of the Standard Model

A calculated pressure transient in the core region and the changing of material distributions are shown in Figs. 4 and 5, respectively. Sodium boiling in the core region occurred at 19.0 s and fuel pin failed at 19.9 s. This fuel-pin failure releases gaseous fission products and the core region is pressurized. Molten-core materials were dispersed toward the lower and upper axial blanket and formed blockages which stopped axial dispersions of core materials. At approximately 21.0 s, the wrapper tube of the fuel subassembly failed and the core pressure decreased. This pressure release became a driving force by which a part of molten-core materials penetrated into the inter-subassembly gap. At approximately 23.0 s, the CRGT failed and the pressure of the core region increased sharply because of a heat transfer from molten-core materials to sodium and resultant rapid vaporization of sodium. Molten fuel did not discharge through CRGT since blockages were formed inside the control-rod subassembly and the dashpot.

2.3 Parametric Calculations

The sharp pressure increase at the CRGT failure is supposed to be rapid sodium vaporization and this pressure increase rate corresponds to heat-transfer rate between the molten-core materials and sodium, namely, the larger pressure increase rate becomes the larger sodium vaporization rate and heat-loss of molten-core materials become. Therefore, a parametric

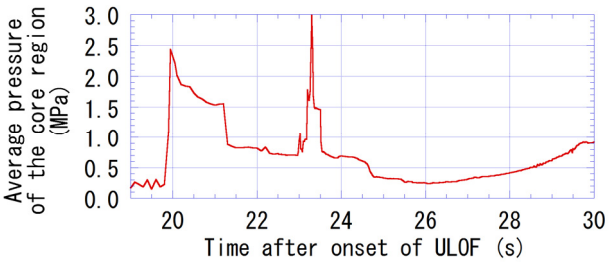

Fig. 4 Pressure transient in the core region.

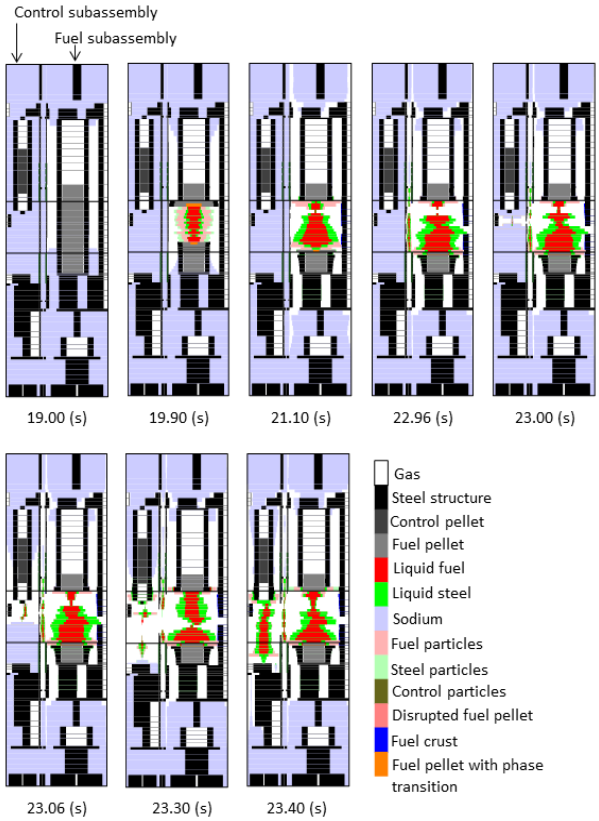

Fig. 5 Changing of material distributions.

calculation was performed in which heat-transfer rate between the molten-core materials and sodium was suppressed. Calculation results for the pressure of core region and changing of material distributions are shown in Figs. 6 and 7, respectively. Pressure did not increase at the CRGT failure and molten fuel discharged through the CRGT since blockages were not formed inside it due to limited heat-loss from the molten-fuel to sodium. This calculation suggests that heat-transfer rate between molten fuel and sodium in the core region is one of dominant phenomena to molten-fuel discharge through the CRGT.

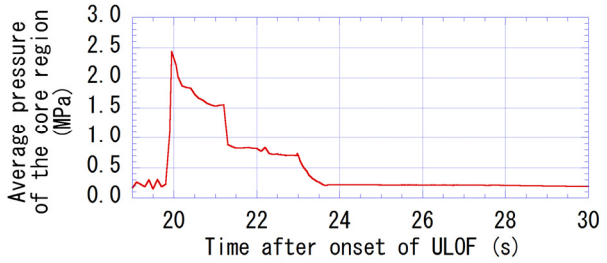

Fig. 6 Pressure transient in the core region (suppressed heat-transfer between molten-core and sodium).

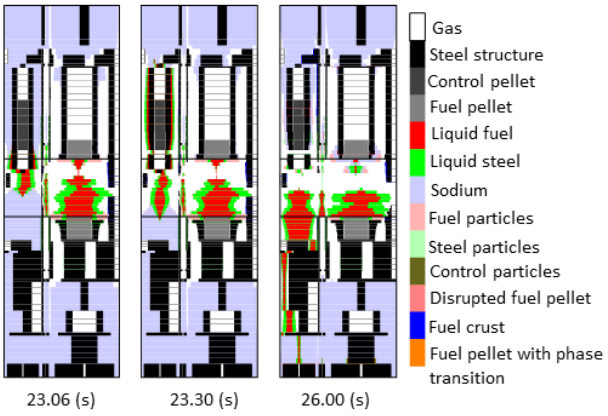

Fig. 7 Changing of material distributions (suppressed heat-transfer between molten-core and sodium).

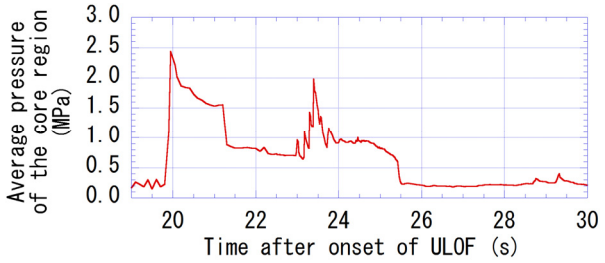

Fig. 8 Pressure transient in the core region (considering occupation of liquid-particle mixture for the cross section).

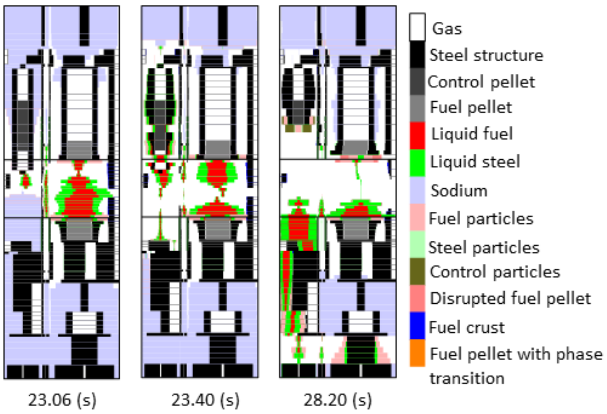

Fig. 9 Changing of material distributions (considering occupation of liquid-particle mixture for the cross section).

Next, a parametric calculation relating to the blockage formation was performed. One can find that, at the position where the blockage is formed in Fig. 5, the cross-section of the CRGT is not completely occupied with fluid-particle mixture. Therefore, a calculation was performed in which the blockage formation was eliminated when the cross-section was not completely occupied with fluid-particle mixture. Calculation results for the pressure of the core region and changing of material distributions are shown in Figs. 8 and 9, respectively. Although the pressure of the core region increased sharply at the CRGT failure, molten-core material discharged through CRGT. This calculation suggests that freezing of molten fuel and blockage formation by frozen fuel inside the CRGT were also identified as dominant phenomena to molten-fuel discharge through the CRGT.

In order to validate the models for describing above the identified phenomena, a series of experimental analyses was implemented, in which molten-fuel simulant discharged through a sodium-filled duct. In next Section 3, model validation and modification are considered through the experimental analyses.

3. Model Validation and Modification

3.1 Summary of the Experiment

An experiment selected for this model validation was executed utilizing an out-of-pile facility at the National Nuclear Center of the Republic of Kazakhstan under the EAGLE (experimental acquisition of generalized logic to eliminate re-criticalities) joint-research program [6]. A schematic diagram of a test section is shown in Fig. 10 with its dimensions. The test section consists of an upper vessel, a discharge duct and a lower vessel, which simulate a degrading core region, a discharge path and a coolant plenum, respectively. Alumina was selected as a fuel simulant. In the experiment, a molten core state was generated by pouring molten alumina into the upper vessel. Approximately 11.6 kg of molten-alumina melted by induction heating atapproximately 2,500 K

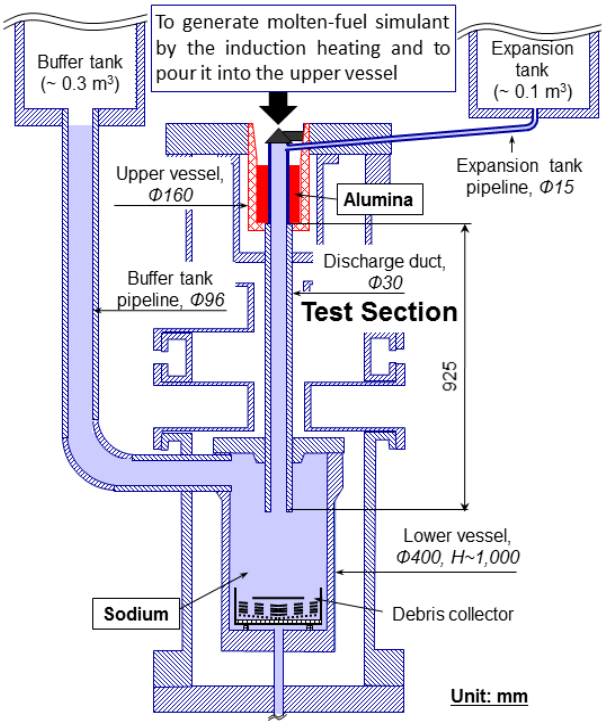

Fig. 10 Schematic of the test section.

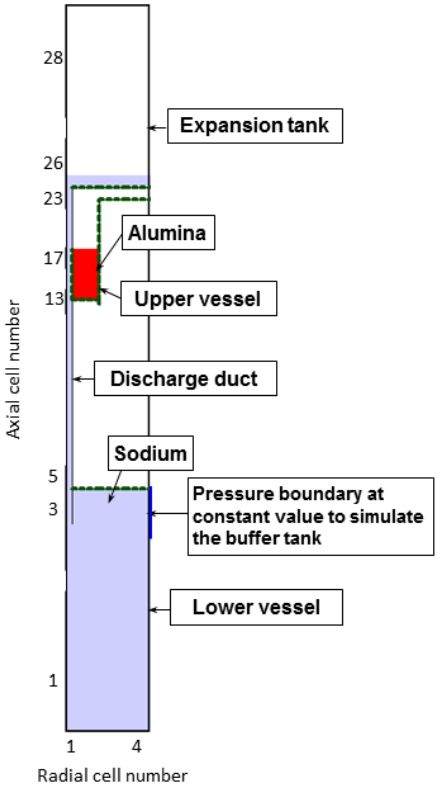

Fig. 11 The model to simulate the experiment.

was poured into the upper vessel, and initial pressures of the upper and lower vessels were 0.34 MPa and 0.14 MPa, respectively. Results of the experiment was summarized that approximately 8.1 kg of alumina was discharged toward the lower vessel during approximately 1.2 s without blockage formation. Approximately 0.8 kg was solidified on the inner surface of the discharge duct and approximately 7.3 kg was discharged into the lower vessel.

3.2 Procedure of Calculations and Results with the Standard Model

In the experimental analyses using the SIMMER-III code, the upper vessel, discharge duct, lower vessel and expansion tank were modeled in a two dimensional geometry as shown in Fig. 11. As the pressure boundary condition, a constant pressure was set in the lower vessel instead of modeling the buffer tank pipeline and buffer tank. Sodium was filled at the bottom of the expansion tank. Pressure conditions for the upper and lower vessels and temperature conditions for molten-alumina, sodium and the discharge duct wall were set in accordance with the initial condition of the experiment.

A calculated result for the cover-gas pressure in the upper vessel is shown in Fig. 12 compared with the experimental result, and results for material distributions are displayed in Fig. 13. It is shown in Fig. 12 that the cover-gas pressure in the upper vessel increased sharply after the penetration of molten-alumina into the discharge duct and that the calculated cover-gas pressure is over-estimated against the experimental result. The material distribution at 2.90 s in Fig. 13 shows that the blockage formation at the lower exit of the discharge duct, and this calculation result is not consistent with the experimental one.

3.3 Model Modification and Application

In order to evaluate the experimental result appropriately, the following three models should be varied: the first is a heat-transfer between

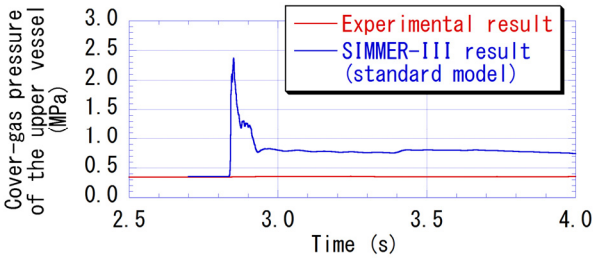

Fig. 12 The cove-gas pressure in the upper vessel.

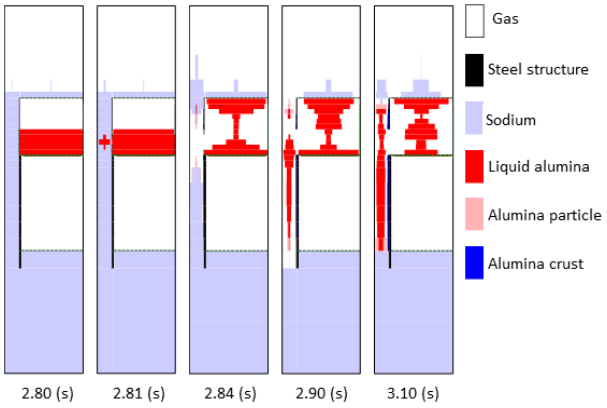

Fig. 13 Changing of material distributions with the standard model.

molten-alumina and sodium; the second is a heat-transfer between molten-alumina and the duct wall, and third is the blockage formation. For the first and second points, the SIMMER-III code employs a non-equilibrium heat-transfer-limited model to evaluate heat and mass transfer at the interface between components 1 and 2 where the net energy transfer rate at the interface, $q^{\mathrm{I}}_{1/2}$ (W·m^{-3}), is described as Eq. (1) [7]:

$$q^{\mathrm{I}}_{1/2} = a^{\mathrm{I}}_{1/2} h_1 \left(T^{\mathrm{I}} - T_1\right) + a^{\mathrm{I}}_{1/2} h_2 \left(T^{\mathrm{I}} - T_2\right) \quad (1)$$

where, $a^{\mathrm{I}}_{1/2}$ (m^{-1}) is an interface area per unit volume between components 1 and 2, h_1 and h_2 (W·m^{-2}·K^{-1}) denote heat transfer coefficients for components 1 and 2, respectively, T^I (K) is the interface temperature between components 1 and 2, and, T_1 and T_2 (K) are temperatures of components 1 and 2, respectively.

When the value of Eq. (1) is zero, sensible heat is exchanged without phase transition at the interface. When the value of Eq. (1) is negative, namely when the energy increases at the interface, either a solid component melts or a liquid component vaporizes. Then the mass transfer rates per unit volume at the interface for melting, $\Gamma^I_{s,L}$ (kg·s^{-1}·m^{-3}), or vaporization, $\Gamma^I_{L,v}$ (kg·s^{-1}·m^{-3}) are determined by the following equation, respectively,

$$\Gamma^I_{s,L} = -\frac{q^I_{1/2}}{i_{liq,L} - i_s} \quad \text{or} \quad \Gamma^I_{L,v} = -\frac{q^I_{1/2}}{i_{sat,v} - i_L} \quad (2)$$

where, i_s (J·kg^{-1}) is specific enthalpy of solid phase component, $i_{liq,L}$ (J·kg^{-1}) is that of liquid phase component at its liquidus point, i_L (J·kg^{-1}) are that of liquid phase component, $i_{sat,v}$ (J·kg^{-1}) is that of saturated vapor.

When the value of Eq. (1) is positive, namely the energy decreases at the interface, either a liquid component freezes or a vapor component condenses. Then the mass transfer rates per unit volume at the interface for freezing, $\Gamma^{\mathrm{I}}_{L,s}$ (kg·s^{-1}·m^{-3}), or condensation, $\Gamma^{\mathrm{I}}_{v,L}$ (kg·s^{-1}·m^{-3}), are determined by the following equation respectively:

$$\Gamma^{\mathrm{I}}_{L,s} = \frac{q^{\mathrm{I}}_{1/2}}{i_L - i_{sol,s}} \quad \text{or} \quad \Gamma^{\mathrm{I}}_{v,L} = \frac{q^{\mathrm{I}}_{1/2}}{i_v - i_{sat,L}} \quad (3)$$

where, $i_{sol,L}$ (J·kg^{-1}) is specific enthalpy of solid phase component at its solidus point, i_v (J·kg^{-1}) is that of vapor phase component and $i_{sat,L}$ (J·kg^{-1}) is that of saturated liquid.

A supposed material distribution at the initiation of molten-alumina penetration into the discharge duct is presented in the left-side of Fig. 14, and the modeling of the SIMMER-III code to treat multi-component heat-transfers is presented in the right side of Fig. 14.

One fluid component which has the largest volume fraction is defined as a continuous phase and other components are defined as a dispersed phase. The dispersed-phase components are modeled as droplets, and the interfacial area between continuous and dispersed phases, $a_{c/d}$, are simply defined by:

$$a_{c/d} = 3\alpha_d / r_d \quad (4)$$

where, α_d and r_d are a volume fraction and a radius of the dispersed phase component, respectively.

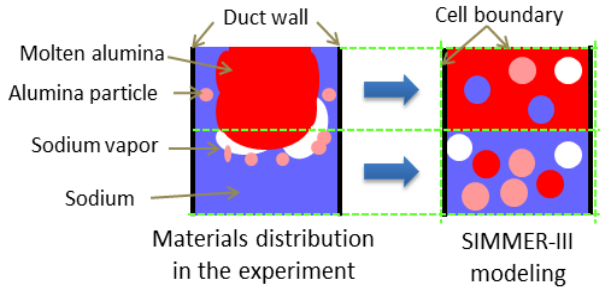

Fig. 14 Comparison of materials distribution at the initiation of molten-alumina penetration into the discharge duct and SIMMER-III modeling.

The radius is assumed to be the maximum stable size of the dispersed phase component governed by the hydrodynamic stability criterion related to a critical Weber number [8].

Applicability of the above models to freezing of molten material and fuel-coolant interactions were confirmed through the assessment studies [5, 8, 9] namely, the heat-transfers from molten material to sodium or the duct wall were verified using experimental data. On the other hand, only few attempts have been made at validation for molten-material discharge through the coolant-filled channel, in which the heat-transfers from the molten material both to sodium and to the channel wall coexist, because of lack of experimental knowledge and databases until execution of the EAGLE program. The present study is the first trial to verify molten-material discharge through the coolant-filled channel using database of the EAGLE program. Eq. (4) shows that the radius of the dispersed phase component determines the interfacial area and, as a result, determines the heat and mass transfer rate as described in Eqs. (1)-(3). The result of the present calculation suggests that the radius of the dispersed phase would be under-estimated at the initiation of melt discharge and that the minimum value of the radius should be limited.

Next, the modification for the blockage formation model is described. In general, when enthalpy of a fluid decreases under its liquidus point, solid nuclei appear in a fluid and its mobility decreases [10]. In the SIMMER-III code, solid nuclei are modeled as solid particles and degradation of fluid mobility is represented by increasing effective viscosity of fluid-particle mixture [4]. As shown in Fig. 13, in the present calculation, the blockage by mixture of liquid alumina and alumina particle was formed at the lower exit of the discharge duct although only a small portion of the cross-section was occupied by this mixture. It is obvious that the blockage is formed when fluid-particle mixture is in contact with the duct wall. Therefore, the blockage formation model should be modified to be coupled with the flow regime map of the multi-phase flow [4, 11]. In other words, the model should be modified so as to form the blockage when mixture of molten-alumina and alumina particles forms the continuous phase.

After modification of the blockage formation model, parametric calculations were performed to find appropriate value for radii of the dispersed components. Calculation results for the cover-gas pressure are presented in Figs. 15 and 16 with the experimental result. These figures suggest that the minimum radius of molten alumina and sodium should be larger than those in the standard model by two and one orders of magnitude, respectively. Changing of material distributions calculated by the modified model is displayed in Fig. 17. In this calculation, minimum radii for molten alumina and sodium are set at 5 mm and 0.5 mm, respectively. It is shown in Fig. 17 that molten alumina discharged through the duct without blockage formation and this calculation results is consistent with the experimental results.

The present results show that the radii of dispersed

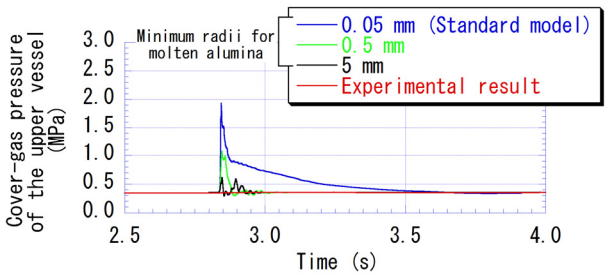

Fig. 15 Effect of minimum radius of molten alumina on the cove-gas pressure in the upper vessel.

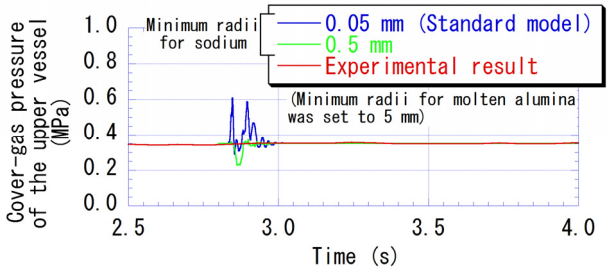

Fig. 16 Effect of minimum radius of sodium on the cove-gas pressure in the upper vessel.

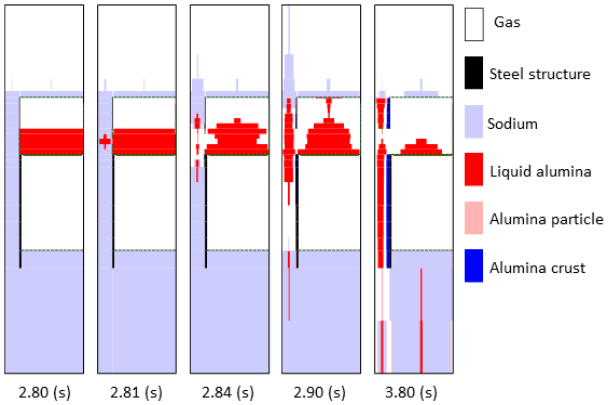

Fig. 17 Changing of material distributions with the modified models.

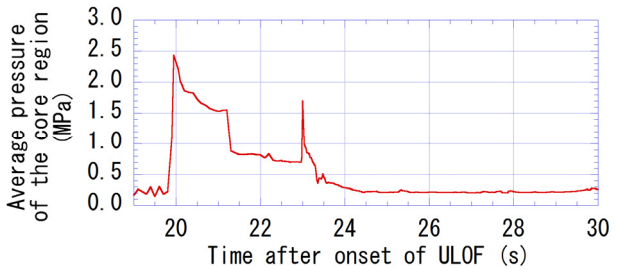

Fig. 18 Pressure transient in the core region evaluated by modified SIMMER-III.

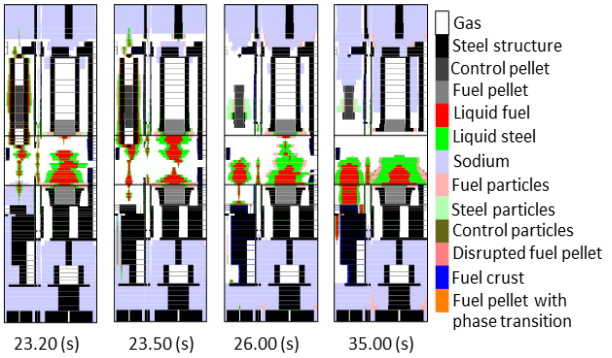

Fig. 19 Changing of material distributions evaluated by modified SIMMER-III.

phase components are one or two orders of magnitude larger than those evaluated by the hydrodynamic stability criterion. Although present knowledge was obtained through the analysis of the experiment using molten alumina and sodium, it can apply to a case in which molten fuel penetrates into the sodium-filled channel since in-pile tests using uranium-dioxide and sodium performed under the EAGLE program showed that pressure increase in the core simulating region at the initiation of fuel discharge was not significant [12, 13]. These experimental evidences support the results of present study and, therefore, the present methodology can be applied to CDA analyses. Needless to say, in order to reinforce this consideration, it is recommended to continue validation studies using the database provided from the in-pile tests.

3.4 Application of Modified SIMMER-III to Fuel-Discharge through the Control Rod Guide Tube

In order to confirm effects of the present model modification on fuel discharge behavior through the CRGT, recalculation of Section 2 was performed using the modified SIMMER-III. A calculated pressure transient in the core region and changing of material distributions are shown in Figs. 18 and 19, respectively. One can confirm from Fig. 19 that molten fuel discharges into the sodium coolant plenum through the CRGT. Although the pressure of the core region increases at the CRGT failure (at approximately 23.0 s) as shown in Fig. 18, its peak value was significantly reduced in comparison with standard model (Fig. 4). The present model modifications show a potential that molten fuel will be effectively discharged from the core region through the CRGT. It should be noted that the core region was also pressurized at the CRGT failure and this pressurization would be one of the driving forces for fuel compacting motion leading to energetics. The pressurization behaviors described above should be further investigated.

4. Conclusions

In the present study, heat-transfer rate between

molten fuel and sodium in the core region, freezing of molten fuel and blockage formation by frozen fuel inside the CRGT were identified as dominant phenomena to molten-fuel discharge through the CRGT. Validations for models of the SIMMER-III code based on experimental evidences required model modifications both on the interface area between molten-fuel and sodium and on the blockage formation. The SIMMER-III code with model modifications could reproduce the experimental results appropriately. Through the present study, the evaluation methodology for the molten-fuel discharge through the CRGT was successfully developed.

Acknowledgments

The present study is the result of "Development of Evaluation Methodology for Core-Material Relocation in Core Disruptive Accidents" entrusted to Japan Atomic Energy Agency by the Ministry of Education, Culture, Sports, Science and Technology of Japan. The authors would also like to express their gratitude to Messrs. S. Hosono and T. Kondo of NESI Inc., for their important technical contributions.

References

[1] A.E. Walter, A.B. Reynolds, Fast Breeder Reactors, Pergamon Press, New York, 1981, pp. 517-525.

[2] T.G. Theofanous, C.R. Bell, An assessment of clinch river breeder reactor core disruptive accident energetics, Nuclear Science and Engineering 93 (1986) 215-228.

[3] K. Morita, S. Kondo, Y. Tobita, N. Shirakawa, D.J. Brear, E.A. Fischer, Computational advances in transition phase analysis, in: Proceedings of International IWGFR Conference on Material-Coolant Interactions and Material Movement and Relocation in Liquid Metal Fast Reactors, O-arai, Ibaraki, Japan, June 6-9, 1994.

[4] H. Yamano, S. Fujita, Y. Tobita, K. Kamiyama, S. Kondo, E.A. Fischer, D.J. Brear, et al., SIMMER-III: a Computer Program for LMFR Core Disruptive Accident Analysis, Version 3.A Model Summary and Program Description, Japan Nuclear Cycle Development Institute Press, Ibaraki, Japan, 2003.

[5] Y. Tobita, S. Kondo, H. Yamano, K. Morita, W. Maschek, P. Coste, et al., The development of SIMMER-III, an advanced computer program for LMFR safety analysis and its application to sodium experiments, Nuclear Technology 153 (3) (2006) 245-255.

[6] K. Kamiyama, M. Saito, K.I. Matsuba, M. Isozaki, I. Sato, K. Konishi, et al., Experimental study on fuel-discharge behaviour through in-core coolant channels, Journal of Nuclear Science and Technology 50 (6) (2013) 629-644.

[7] K. Morita, H. Yamano, Y. Tobita, S. Kondo, SIMMER-III/IV Heat- and Mass-Transfer Model—Model and Method Description, Japan Nuclear Cycle Development Institute Press, Ibaraki, Japan, 2003.

[8] K. Morita, Sa Kondo, Y. Tobita, D.J. Brear, SIMMER-III applications to fuel-coolant interactions, Nuclear Engineering and Design 189 (1999) 337-357.

[9] K. Kamiyama, D.J. Brear, Y. Tobita, S. Kondo, Establishment of freezing model for reactor safety analysis, Journal of Nuclear Science and Technology 43 (10) (2006) 1206-1217.

[10] W. Kurz, D.J. Fisher, Fundamentals of Solidification, 3rd ed., Trans Tech Publications, Dürnten, Switzerland, 1992, pp. 1-17.

[11] Y. Tobita, K. Morita, S. Kondo, N. Shirakawa, Interfacial area modeling for a multiphase, multicomponent fluid-dynamics code, in: Proceedings of the International Conference on Multiphase Flows '91-Tsukuba, Tsukuba, Japan, Sept. 24-27, 1991.

[12] K. Konishi, S. Kubo, I. Sato, K. Koyama, J.I. Toyooka, K. Kamiyama, et al., The eagle project to eliminate the recriticality issue of fast reactors—progress and results of in-pile tests, in: Proceedings of NTHAS5, Jeju, Korea, Nov. 26-29, 2006.

[13] K. Kamiyama, K. Konishi, I. Sato, J. Toyooka, K. Matsuba, V.A. Zuyev et al., Experimental studies on upward fuel discharge during core disruptive accident in sodium-cooled fast reactors, in: Proceedings of NTHAS8, Beppu, Japan, Dec. 9-12, 2012.